

Article

# Highly Sensitive and Selective Colorimetric Detection of Methylmercury Based on DNA Functionalized Gold Nanoparticles

Zheng-Jun Xie <sup>1,2</sup>, Xian-Yu Bao <sup>2,3</sup> and Chi-Fang Peng <sup>1,2,\*</sup> 

<sup>1</sup> State Key Laboratory of Dairy Biotechnology, Shanghai Engineering Research Center of Dairy Biotechnology, Dairy Research Institute, Bright Dairy & Food Co., Ltd., Shanghai 200436, China; xiejz@jiangnan.edu.cn

<sup>2</sup> School of Food Science and Technology, Jiangnan University, Wuxi 214122, China; 6150111037@vip.jiangnan.edu.cn

<sup>3</sup> Shenzhen Academy of Inspection and Quarantine, Shenzhen 518045, China

\* Correspondence: pcf@jiangnan.edu.cn; Tel.: +86-510-8591-9189

Received: 11 June 2018; Accepted: 30 July 2018; Published: 15 August 2018



**Abstract:** A new colorimetric detection of methylmercury ( $\text{CH}_3\text{Hg}^+$ ) was developed, which was based on the surface deposition of Hg enhancing the catalytic activity of gold nanoparticles (AuNPs). The AuNPs were functionalized with a specific DNA strand ( $\text{H}_{17}$ ) recognizing  $\text{CH}_3\text{Hg}^+$ , which was used to capture and separate  $\text{CH}_3\text{Hg}^+$  by centrifugation. It was found that the  $\text{CH}_3\text{Hg}^+$  reduction resulted in the deposition of Hg onto the surface of AuNPs. As a result, the catalytic activity of the AuNPs toward the chromogenic reaction of 3,3',5,5'-tetramethylbenzidine (TMB)- $\text{H}_2\text{O}_2$  was remarkably enhanced. Under optimal conditions, a limit of detection of 5.0 nM was obtained for  $\text{CH}_3\text{Hg}^+$  with a linear range of 10–200 nM. We demonstrated that the colorimetric method was fairly simple with a low cost and can be conveniently applied to  $\text{CH}_3\text{Hg}^+$  detection in environmental samples.

**Keywords:** methylmercury; gold nanoparticles; enzyme mimic; chromogenic reaction

## 1. Introduction

Mercuric ions widely exist in the environment and have distinct toxic effects on human beings. Organic forms of mercury (Hg) demonstrate much higher toxicity than inorganic Hg due to their higher lipophilicity and easier bioaccumulation through the food chain, such as in the tissue of fish [1,2]. The main organic species of mercury, methylmercury ( $\text{CH}_3\text{Hg}^+$ ), has been recognized as a potent neurotoxin that causes damage to the brain and nervous system [1,3]. Due to the severe effects of mercury, the U.S. Environmental Protection Agency has set a maximum level (10 nM, 2 ppb) for mercury species in drinking water [1]. Usually, complex hyphenated techniques, such as high performance liquid chromatography (HPLC) or gas chromatography (GC), coupled to specific detectors, such as mass spectrometry (MS), inductively coupled plasma mass spectrometry (ICP-MS) or atomic fluorescence spectrometry (AFS), are required for methylmercury detection [4–6]. However, these techniques generally require expensive instruments and are time-consuming and costly. To overcome the limitation of the above methods, recently, nanomaterial-based assays have been widely used for developing rapid and cost-effective methods for the detection of various heavy metal ions in environmental and biological samples [7–9]. Due to the strong metallophilic interactions between  $\text{Hg}^{2+}$  and some other metallic atoms, such as gold and silver, numerous metallic nanoparticle-based assays for  $\text{Hg}^{2+}$  have been developed [10–16]. However, there are fewer nanomaterial-based assays for  $\text{CH}_3\text{Hg}^+$  compared to  $\text{Hg}^{2+}$  ions [17–19], which is probably due to the weak interactions between  $\text{CH}_3\text{Hg}^+$  and metal nanomaterials.

Only a few studies have reported the development of nanomaterial-based detection methods for  $\text{CH}_3\text{Hg}^+$ . For example, Chen et al. developed a colorimetric nanosensor for mercury speciation, which was based on the analyte-induced aggregation of gold nanoparticles (Au NPs) with the assistance of a thiol-containing ligand of diethyldithiocarbamate (DDTC) [18]. Pandeewar et al. presented a novel optoelectronic approach for detection of  $\text{Hg}^{2+}$  and  $\text{CH}_3\text{Hg}^+$ , which was based on nanoarchitectonics that consists of an adenine (A)-conjugated small organic semiconductor (BNA) and deoxyribo-oligothymidine (dTn) [20]. However, this device cannot distinguish  $\text{Hg}^{2+}$  from  $\text{CH}_3\text{Hg}^+$ . Recently, Deng et al. reported that a DNA strand,  $\text{H}_{17}$ , can bind to  $\text{CH}_3\text{Hg}^+$  with a higher  $K_b$  value of  $(5.57 \pm 0.47) \times 10^6 \text{ M}^{-1}$  compared to that of  $\text{Hg}^{2+}$  ( $(1.51 \pm 0.18) \times 10^6 \text{ M}^{-1}$ ) [19]. Based on this, they were able to discriminate between  $\text{CH}_3\text{Hg}^+$  and  $\text{Hg}^{2+}$  ions by forming Ag/Hg amalgam with a  $\text{CH}_3\text{Hg}^+$ -specific fluorophore-labeled DNA probe and fabricated a highly selective fluorescent assay for  $\text{CH}_3\text{Hg}^+$ . More recently, Yang et al. designed a specific visual detection method for  $\text{CH}_3\text{Hg}^+$  and ethylmercury based on DNA-templated alloy Ag/Au NPs [21]. However, this visual detection method for methylmercury and ethylmercury requires subtle temperature adjustments and its sensitivity was above the micromolar level. Thus, developing a simple and selective colorimetric assay for  $\text{CH}_3\text{Hg}^+$  is still an important and difficult task.

Recently, some methods for the detection of  $\text{Hg}^{2+}$  were reported, which were based on the peroxidase-like activity of the AuHg alloy NPs. For example, Long et al. [22] found that AuNPs possess excellent peroxidase-like activity after the deposition of  $\text{Hg}^{2+}$  onto the surface of AuNPs. The peroxidase-like activity enhancement of AuNPs, after  $\text{Hg}^0$  deposition onto the surface of AuNPs, was suggested to be the result of the accelerated decomposition of  $\text{H}_2\text{O}_2$  and the stabilization of hydroxyl radicals on the surface of AuNPs. This phenomenon can be applied in the development of colorimetric and fluorescent assays for  $\text{Hg}^{2+}$  [22–24]. Our group also reported that catalytic DNA-AuNPs and DNA-Ag/Pt nanoclusters can be used to detect  $\text{Hg}^{2+}$  with high selectivity and sensitivity by stimulating or inhibiting their peroxidase-like activity [25,26]. Interestingly, compared with citrate stabilized AuNPs, AuNPs functionalized with a T-rich DNA strand can obviously improve the selectivity and can simplify the sample pretreatment for the colorimetric detection of  $\text{Hg}^{2+}$  [25]. However, to the best of our knowledge, there is no report on the application of nanomaterial enzyme mimics in  $\text{CH}_3\text{Hg}^+$  detection. Herein, we found that  $\text{CH}_3\text{Hg}^+$  captured by the AuNPs functionalized with  $\text{CH}_3\text{Hg}^+$ -specific DNA strands can be reduced by  $\text{NaBH}_4$ . This results in Hg deposition onto the surface of AuNPs, thus stimulating the peroxidase-like activity of the AuNPs. Based on this finding, a highly sensitive and selective colorimetric assay for  $\text{CH}_3\text{Hg}^+$  was developed.

## 2. Materials and Methods

### 2.1. Chemicals and Materials

$\text{HAuCl}_4$ ,  $\text{CH}_3\text{Hg}^+\text{Cl}$ ,  $\text{NaBH}_4$ , 3,3',5,5'-Tetramethylbenzidine (TMB) and  $\text{H}_2\text{O}_2$  (30%) were purchased from Aladdin Reagent (Shanghai, China). The single-strand oligonucleotides were obtained from Sangon Biotech (Shanghai, China) and the sequences of these DNA strands were listed in Table 1.  $\text{Hg}(\text{NO}_3)_2$  and all the other metal salts were purchased from the National Institute of Metrology (Beijing, China). All of the reagents used were of analytical grade. Ultra-pure water prepared with a Milli-Q Pure system was used for all experiments.

**Table 1.** Oligonucleotide Sequences Used in This Work <sup>a</sup>.

Type	Sequence
H <sub>T5</sub>	5'-SH-CTTGTGTTAAAAATTCTTTG-3'
H <sub>T7</sub>	5'-SH-GTTCTTGTGTTAAAAATTCTTTGTTC-3'
H <sub>T9</sub>	5'-SH-TTGTTCCTTGTGTTAAAAATTCTTTGTTCTT-3'
H <sub>R</sub>	5'-SH-CTGCTGCTGCAAAAAGCAGCAGCAG-3'

<sup>a</sup> H<sub>T5</sub>, H<sub>T7</sub> and H<sub>T9</sub> represent CH<sub>3</sub>Hg<sup>+</sup>-specific DNA with different T bases, while H<sub>R</sub> represents random DNA.

## 2.2. Synthesis of AuNPs and the Modification by DNA Strands

The AuNPs were prepared through the citrate-mediated reduction of HAuCl<sub>4</sub> [24]. Briefly, HAuCl<sub>4</sub> (0.01%, 100 mL) was added to a flask, which had been washed with aqua regia and ultra-pure water. After the solution was heated to boiling, sodium citrate (1.0%, 2.0 mL) was quickly added with stirring. When we observed a color change in the mixture to wine red, the mixture was further boiled for another 5 min and cooled to room temperature. The diameter of AuNPs was about 15 nm and their concentration was estimated to be 3 nM.

The DNA modification of the AuNPs was achieved by directly incubating thiolated single-strand DNA (H<sub>T7</sub>) with the AuNPs. Briefly, the AuNPs (3 nM, 990 μL) and thiolated DNA (100 μM, 5 μL) were mixed together and incubated at an ambient temperature for 24 h. After this, the mixture was centrifuged for 15 min at 10,000 × g rpm and excessive DNA strands were removed. After repeating the centrifugation once, the obtained DNA-AuNPs complex was resuspended in phosphate buffer (10 mM, pH of 7.0) and stored at 4 °C.

## 2.3. Colorimetric Detection of CH<sub>3</sub>Hg<sup>+</sup>

To 25 μL of DNA-AuNPs complex (0.6 nM), 175 μL of Tris-HNO<sub>3</sub> buffer (5.0 mM, pH 7.0) and 500 μL of CH<sub>3</sub>Hg<sup>+</sup> solution at different concentrations were added. After being incubated for 10 min, the mixtures were centrifuged at 10,000 rpm for 15 min and the supernatants were discarded. To the 50 μL of retained mixture, we added 50 μL of NaBH<sub>4</sub> (1.0 mM). After being incubated for another 10 min, 90 μL of citrate buffer (100 mM, pH 4.5), 100 μL of TMB (1.5 mM) and 60 μL of H<sub>2</sub>O<sub>2</sub> (1.5 M) were transferred into the solution. The catalytic reaction was subsequently recorded at 650 nm by a microplate reader (PowerWave XS<sub>2</sub>, Bio-Tek, Winooski, VT, USA) after 10 min. For detection of CH<sub>3</sub>Hg<sup>+</sup> in lake water, the samples were filtered through microfiltration membranes and measured by the above method.

## 3. Results and Discussion

### 3.1. Characterization of AuNPs and DNA-AuNPs Complex

Figure 1 shows that the UV-vis absorption spectra of the AuNPs has a maximum absorption peak ( $\lambda_{\max}$ ) at 520 nm. After the AuNPs were modified with H<sub>T7</sub>, which is a CH<sub>3</sub>Hg<sup>+</sup> recognition DNA strand, the  $\lambda_{\max}$  of the AuNPs experienced a red shift to 522 nm. This result suggested that the DNA-AuNPs complex (H<sub>T7</sub>-AuNPs) was obtained. The H<sub>T7</sub>-AuNPs complex was stable in 0.15 M NaCl (the inset in Figure 1), which also indicated the successful preparation of the H<sub>T7</sub>-AuNPs.

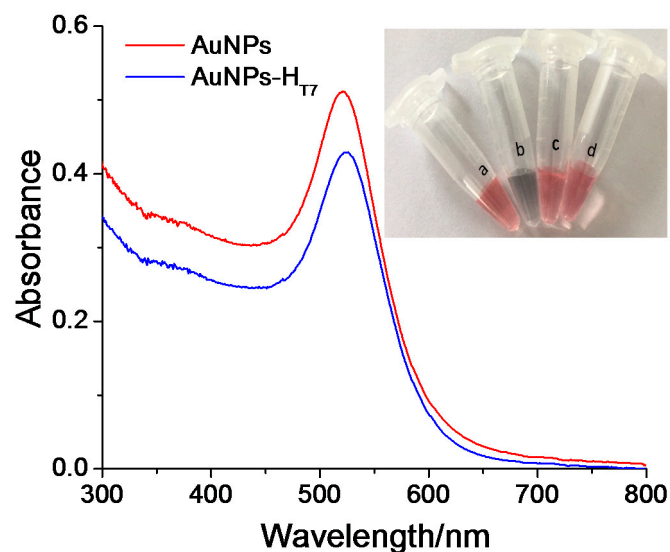


**Figure 1.** UV-vis spectra of AuNPs and AuNPs-H<sub>T7</sub>. The inset shows the photographs of (a) AuNPs, (b) AuNPs with 0.15 mol/L NaCl, (c) AuNPs-H<sub>T7</sub> and (d) AuNPs-H<sub>T7</sub> with 0.15 mol/L NaCl.

### 3.2. Colorimetric Detection of CH<sub>3</sub>Hg<sup>+</sup>

As shown in Figure 2, AuNPs-H<sub>T7</sub> demonstrated weak catalytic activity and we only found a weak signal with a peak at 650 nm. After being captured by the H<sub>T7</sub> strand, CH<sub>3</sub>Hg<sup>+</sup> species can be deposited onto the surface of AuNPs through Au/Hg amalgamation since they can be reduced to Hg<sup>0</sup> by NaBH<sub>4</sub> [19,27,28]. In the above process, the catalytic activity of AuNPs-H<sub>T7</sub> was obviously increased, which was supported by the appearance of a strong signal at 650 nm. This was due to the oxidation of TMB by the hydroxyl radical that is stabilized on the surface of AuNPs, which produces a blue one-electron oxidation product (i.e., cation free-radical, TMB<sup>•+</sup>) [29]. The reaction is shown in Figure S1. This change in peroxidase-like activity of the AuNPs suggests the deposition of Hg onto the surface of AuNPs [22,25]. The CH<sub>3</sub>Hg<sup>+</sup> sensing mechanism is depicted in Scheme 1.

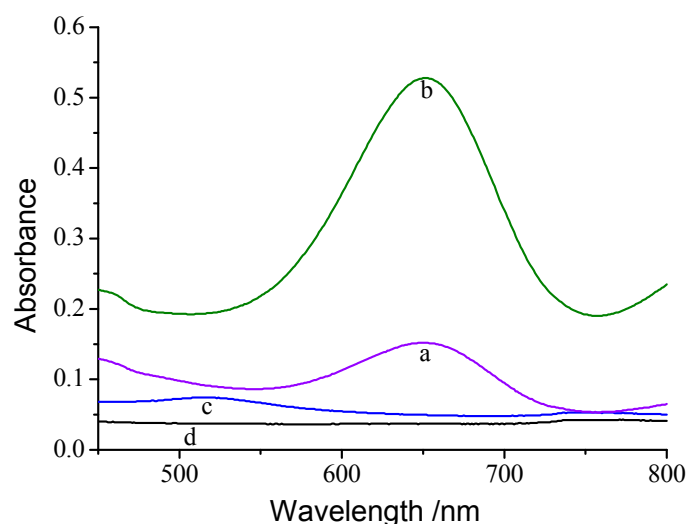
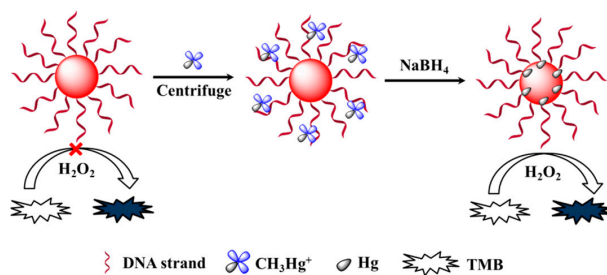


**Figure 2.** UV-vis spectra of AuNPs-H<sub>T7</sub> + TMB-H<sub>2</sub>O<sub>2</sub> reaction solution (a) before and (b) after capturing CH<sub>3</sub>Hg<sup>+</sup> and Hg deposition, (c) AuNPs-H<sub>T7</sub> solution and (d) TMB-H<sub>2</sub>O<sub>2</sub> substrate.



**Scheme 1.**  $\text{CH}_3\text{Hg}^+$  sensing mechanism.

Since the number of T-T pairs may affect the response of the AuNPs-ssDNA complex to  $\text{CH}_3\text{Hg}^+$ ,  $\text{H}_{\text{T}5}$ ,  $\text{H}_{\text{T}7}$  and  $\text{H}_{\text{T}9}$  strands were used to modify the AuNPs, respectively, before we carried out a comparison of these AuNPs-ssDNA complexes. These AuNPs-ssDNA complexes were also characterized by UV-vis spectra, which demonstrated the same change compared with the AuNPs. As shown in Figure 3,  $\text{H}_{\text{T}7}$  modified AuNPs demonstrated more sensitive responses to  $\text{CH}_3\text{Hg}^+$  compared to  $\text{H}_{\text{T}5}$ ,  $\text{H}_{\text{T}9}$  or  $\text{H}_{\text{R}}$  modified AuNPs. This result suggested that the higher affinity of DNA strand to  $\text{CH}_3\text{Hg}^+$  over  $\text{Hg}^{2+}$  was still the main factor determining the selectivity of this probe [19].

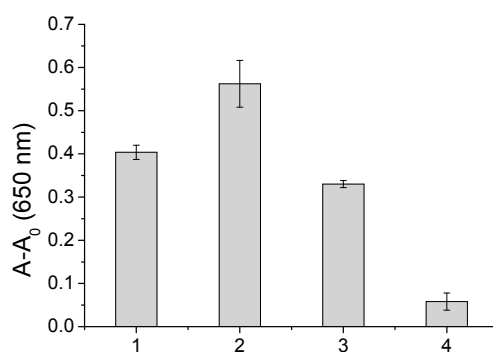


**Figure 3.** Effect of DNA sequence on the colorimetric detection for  $\text{CH}_3\text{Hg}^+$ . AuNPs, 0.6 nM;  $\text{CH}_3\text{Hg}^+$ , 100 nM. TMB,  $1.0 \times 10^{-3}$  M;  $\text{H}_2\text{O}_2$ , 1.5 M; pH, 4.5; and incubation time, 25 min.

The enhanced peroxidase-like activity of AuNPs caused by  $\text{CH}_3\text{Hg}^+$  was further applied in the development of a colorimetric assay for  $\text{CH}_3\text{Hg}^+$ . As shown in Figure 4, the absorbance increased as the  $\text{CH}_3\text{Hg}^+$  concentration increased in the range of 0–1000 nM. A good linear relationship between  $\text{CH}_3\text{Hg}^+$  concentration and absorbance values can be obtained in the range of 10–200 nM. The limit of detection (3-fold signal to noise,  $S/N = 3$ ) was evaluated to be 5.0 nM.

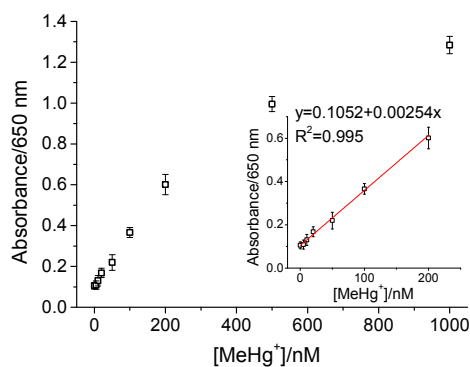


**Figure 4.** Calibration curve for the detection of  $\text{CH}_3\text{Hg}^+$ . AuNPs,  $6.0 \times 10^{-10}$  M; TMB,  $1.5 \times 10^{-3}$  M;  $\text{H}_2\text{O}_2$ , 1.5 M;  $\text{Hg}^{2+}$ ,  $4.0 \times 10^{-7}$  M; pH, 4.4; and incubation time, 20 min.

Some common metal ions were tested in this colorimetric assay. As shown in Figure 5, most of common metal ions at a 20-fold higher concentration and the same concentration of  $\text{Hg}^{2+}$  showed very weak responses. On the contrary, when citrate-stabilized AuNPs were incubated with  $\text{Hg}^{2+}$  or  $\text{CH}_3\text{Hg}^+$  ions, almost the same catalytic enhancement of AuNPs was observed (Figure S2). The above results clearly demonstrated the good selectivity of this colorimetric assay for  $\text{CH}_3\text{Hg}^+$ , which was mainly due to the two aspects: (1)  $\text{CH}_3\text{Hg}^+$ -specific DNA scaffold has much higher affinity to  $\text{CH}_3\text{Hg}^+$  (a  $K_b$  value of  $(5.57 \pm 0.47) \times 10^6 \text{ M}^{-1}$ ) compared to  $\text{Hg}^{2+}$  ( $(1.51 \pm 0.18) \times 10^6 \text{ M}^{-1}$ ); and (2) the centrifugation and separation of AuNPs- $\text{H}_{\text{T}7}$  enriched  $\text{CH}_3\text{Hg}^+$  over  $\text{Hg}^{2+}$ . It also should be pointed out that  $\text{Hg}^{2+}$  has good affinity with AuNPs. However, the DNA strand on the AuNPs will interact with  $\text{Hg}^{2+}$  and thus, will eventually affect the deposition of  $\text{Hg}^0$ . In this case, the  $\text{H}_{\text{T}7}$  strands probably hindered the deposition of  $\text{Hg}^{2+}$ .

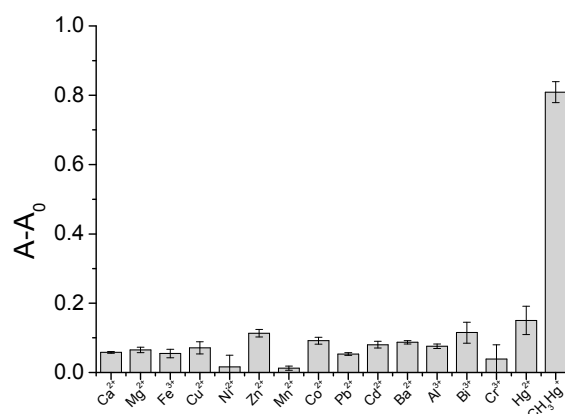


Figure 5. Selectivity of the colorimetric assay for  $\text{CH}_3\text{Hg}^+$ .

The sensitivity of the proposed method was higher than the two typical colorimetric methods [18,21] and comparable with some typical nanosensors or chemosensors (Table 2) [1,17,30,31]. However, the selectivity of this method needs to be further improved when compared with the established colorimetric [21] and fluorescent methods [19,30].

The real water samples from the Li Lake in Wuxi, Jiangsu Province were obtained and spiked with different concentrations of  $\text{CH}_3\text{Hg}^+$  (20 nM, 50 nM and 100 nM). As shown in Table 3, the recovery of the added  $\text{CH}_3\text{Hg}^+$  with the colorimetric method was in the range of 93.6–102.1%, which demonstrated the reliability of this assay for the detection of  $\text{CH}_3\text{Hg}^+$  in real samples.

**Table 2.** Summarize of some typical method of  $\text{CH}_3\text{Hg}^+$ .

Method	Probe	Limit of Detection	Linear Range	Selectivity to $\text{Hg}^{2+}$	Sample	Ref.
Fluorescent	Lys VI-AuNCs	$\text{CH}_3\text{Hg}^+$ : 3 pM $\text{Hg}^{2+}$ : 4 nM	$\text{CH}_3\text{Hg}^+$ : 15–500 nM; $\text{Hg}^{2+}$ : 10–5000 pM		seawater	[1]
Upconversion fluorescence	hCy7-UCNPs	0.8 ppb	0–7 $\mu\text{M}$ ;	Not clear	cells	[17]
Colorimetric	Diethyldithiocarbamate-AuNPs	$\text{CH}_3\text{Hg}^+$ : 15 nM $\text{Hg}^{2+}$ : 10 nM	$\text{CH}_3\text{Hg}^+$ : 0.03–0.8 $\mu\text{M}$ ; $\text{Hg}^{2+}$ : 0.01–0.1 $\mu\text{M}$	EDTA can mask $\text{Hg}^{2+}$	drinking water	[18]
Fluorescent sensing by in-situ synthesis	carbon dots	5.9 nM	23–278 nM	tolerate with 250-fold $\text{Hg}^{2+}$	River/sea water <sup>a</sup>	[30]
Fluorescent sensing by in-situ synthesis	Silver nanocluster	0.4 nM	2.0 nM–12.0 $\mu\text{M}$	tolerate with 50-fold $\text{Hg}^{2+}$	Fish sample	[19]
chiro-optical	adenine -small organic semiconductor and oligothymidine	$\text{CH}_3\text{Hg}^+/\text{Hg}^{2+}$ : 0.1 nM	1–1000 nM	-	water	[20]
AIE-based fluorescence	tetraphenylethylene-monoboronic acid	$\text{CH}_3\text{Hg}^+/\text{Hg}^{2+}$ : 0.12 ppm	0.6–30 ppm	-	Fish muscle	[31]
Colorimetric	DNA-Templated Ag–Au nanoparticles synthesis	0.5 $\mu\text{M}$	0–200 $\mu\text{M}$	tolerate with 50-fold $\text{Hg}^{2+}$	Fish muscle	[21]
Colorimetric	DNA-AuNPs	5 nM	20–500 nM	tolerate with 1-fold $\text{Hg}^{2+}$	Lake water	This work

<sup>a</sup> cleanup using C18 cartridges.

**Table 3.** Detection of CH<sub>3</sub>Hg<sup>+</sup> in real water samples (n = 3).

Water Sample	Added (nM)	Mean Found (nM)	Mean Recovery (%)
1	20	19.1 ± 0.9	95.5%
2	50	46.8 ± 2.3	93.6%
3	100	102.1 ± 3.7	102.1%

#### 4. Conclusions

In summary, we developed a highly sensitive and selective colorimetric method for the detection of CH<sub>3</sub>Hg<sup>+</sup>, which was based on the surface deposition of Hg enhancing the catalytic activity of AuNPs. The limit of detection was 5.0 nM with a linear range of 10–200 nM. This colorimetric method has potential in the detection of CH<sub>3</sub>Hg<sup>+</sup> in environmental samples since it also demonstrated other advantages of being simple, rapid and cost-effective. However, this method needs to be further improved with respect to its selectivity to Hg<sup>2+</sup>. This probably can be further improved through adopting magnetic core gold shell nanocomposites due to their more convenient separation and enrichment capability.

**Supplementary Materials:** The following are available online at <http://www.mdpi.com/1424-8220/18/8/2679/s1>, Figure S1. Chromogenic reaction of TMB; Figure S2. UV–vis spectra of citrate-stabilized AuNPs + TMB-H<sub>2</sub>O<sub>2</sub> reaction solution.

**Author Contributions:** Z.-J.X. mainly run the experiments, X.-Y.B. provided some reagents and participated in the draft writing, and C.-F.P. conceived and designed the experiments.

**Funding:** This research was funded by the Open Project Program of State Key Laboratory of Dairy Biotechnology, Bright Dairy & Food Co. Ltd. (SKLDB2017-00) and the Science and Technology Innovation Committee of Shenzhen (CXZZ20140419150802007), the National Natural Science Foundation of China (31371767).

**Conflicts of Interest:** The authors declare no conflict of interest.

#### References

- Lin, Y.-H.; Tseng, W.-L. Ultrasensitive Sensing of Hg<sup>2+</sup> and CH<sub>3</sub>Hg<sup>+</sup> Based on the Fluorescence Quenching of Lysozyme Type VI-Stabilized Gold Nanoclusters. *Anal. Chem.* **2010**, *82*, 9194–9200. [[CrossRef](#)] [[PubMed](#)]
- Liu, D.B.; Qu, W.S.; Chen, W.W.; Zhang, W.; Wang, Z.; Jiang, X.Y. Highly Sensitive, Colorimetric Detection of Mercury(II) in Aqueous Media by Quaternary Ammonium Group-Capped Gold Nanoparticles at Room Temperature. *Anal. Chem.* **2010**, *82*, 9606–9610. [[CrossRef](#)] [[PubMed](#)]
- Myers, G.J.; Marsh, D.O.; Davidson, P.W.; Cox, C.; Shamlaye, C.F.; Tanner, M.; Choi, A.; Cernichiari, E.; Choisy, O.; Clarkson, T.W. Main neurodevelopmental study of Seychellois children following in utero exposure to methylmercury from a maternal fish diet: Outcome at six months. *Neurotoxicology* **1995**, *16*, 653–664. [[PubMed](#)]
- Hight, S.C.; Cheng, J. Determination of methylmercury and estimation of total mercury in seafood using high performance liquid chromatography (HPLC) and inductively coupled plasma-mass spectrometry (ICP-MS): Method development and validation. *Anal. Chim. Acta* **2006**, *567*, 160–172. [[CrossRef](#)]
- Vallant, B.; Kadnar, R.; Goessler, W. Development of a new HPLC method for the determination of inorganic and methylmercury in biological samples with ICP-MS detection. *J. Anal. At. Spectrom.* **2007**, *22*, 322–325. [[CrossRef](#)]
- Gao, Y.; Galan, S.D.; Brauwere, A.D.; Baeyens, W.; Leermakers, M. Mercury speciation in hair by headspace injection–gas chromatography–atomic fluorescence spectrometry (methylmercury) and combustion-atomic absorption spectrometry (total Hg). *Talanta* **2010**, *82*, 1919–1923. [[CrossRef](#)] [[PubMed](#)]
- Priyadarshini, E.; Pradhan, N. Gold nanoparticles as efficient sensors in colorimetric detection of toxic metal ions: A review. *Sens. Actuators B Chem.* **2017**, *238*, 888–902. [[CrossRef](#)]
- Mao, S.; Chang, J.; Zhou, G.; Chen, J. Nanomaterial-enabled Rapid Detection of Water Contaminants. *Small* **2015**, *11*, 5336–5359. [[CrossRef](#)] [[PubMed](#)]
- Mehta, J.; Bhardwaj, S.K.; Bhardwaj, N.; Paul, A.K.; Kumar, P.; Kim, K.H.; Deep, A. Progress in the biosensing techniques for trace-level heavy metals. *Biotechnol. Adv.* **2016**, *34*, 47–60. [[CrossRef](#)] [[PubMed](#)]

10. Chen, L.; Li, J.; Chen, L.X. Colorimetric Detection of Mercury Species Based on Functionalized Gold Nanoparticles. *ACS Appl. Mater. Interfaces* **2014**, *6*, 15897–15904. [[CrossRef](#)] [[PubMed](#)]
11. Sener, G.; Uzun, L.; Denizli, A. Lysine-Promoted Colorimetric Response of Gold Nanoparticles: A Simple Assay for Ultrasensitive Mercury(II) Detection. *Anal. Chem.* **2014**, *86*, 514–520. [[CrossRef](#)] [[PubMed](#)]
12. Jin, L.H.; Han, C.S. Eco-friendly colorimetric detection of mercury(II) ions using label-free anisotropic nanogolds in ascorbic acid solution. *Sens. Actuators B Chem.* **2014**, *195*, 239–245. [[CrossRef](#)]
13. Liu, H.; Ma, L.; Ma, C.; Du, J.; Wang, M.; Wang, K. Quencher-Free Fluorescence Method for the Detection of Mercury(II) Based on Polymerase-Aided Photoinduced Electron Transfer Strategy. *Sensors* **2016**, *16*, 1945. [[CrossRef](#)] [[PubMed](#)]
14. Xiao, W.; Xiao, M.; Fu, Q.; Yu, S.; Shen, H.; Bian, H.; Tang, Y. A Portable Smart-Phone Readout Device for the Detection of Mercury Contamination Based on an Aptamer-Assay Nanosensor. *Sensors* **2016**, *16*, 1871. [[CrossRef](#)] [[PubMed](#)]
15. Kamaruddin, N.; Bakar, A.A.; Mobarak, N.; Zan, M.S.; Arsad, N. Binding Affinity of a Highly Sensitive Au/Ag/Au/Chitosan-Graphene Oxide Sensor Based on Direct Detection of Pb<sup>2+</sup> and Hg<sup>2+</sup> Ions. *Sensors* **2017**, *17*, 2277. [[CrossRef](#)] [[PubMed](#)]
16. Wang, G.L.; Zhu, X.Y.; Jiao, H.J.; Dong, Y.M.; Li, Z.J. Ultrasensitive and dual functional colorimetric sensors for mercury (II) ions and hydrogen peroxide based on catalytic reduction property of silver nanoparticles. *Biosens. Bioelectron.* **2012**, *31*, 337–342. [[CrossRef](#)] [[PubMed](#)]
17. Liu, Y.; Chen, M.; Cao, T.; Sun, Y.; Li, C.; Liu, Q.; Yang, T.; Yao, L.; Feng, W.; Li, F. A cyanine-modified nanosystem for in vivo upconversion luminescence bioimaging of methylmercury. *J. Am. Chem. Soc.* **2013**, *135*, 9869–9876. [[CrossRef](#)] [[PubMed](#)]
18. Chen, L.; Li, J.; Chen, L. Colorimetric detection of mercury species based on functionalized gold nanoparticles. *ACS Appl. Mater. Interfaces* **2014**, *6*, 15897–15904. [[CrossRef](#)] [[PubMed](#)]
19. Deng, L.; Li, Y.; Yan, X.; Xiao, J.; Ma, C.; Zheng, J.; Liu, S.; Yang, R. Ultrasensitive and highly selective detection of bioaccumulation of methyl-mercury in fish samples via Ag<sup>0</sup>/Hg<sup>0</sup> amalgamation. *Anal. Chem.* **2015**, *87*, 2452–2458. [[CrossRef](#)] [[PubMed](#)]
20. Pandeewar, M.; Senanayak, S.P.; Govindaraju, T. Nanoarchitectonics of Small Molecule and DNA for Ultrasensitive Detection of Mercury. *ACS Appl. Mater. Interfaces* **2016**, *8*, 30362–30371. [[CrossRef](#)] [[PubMed](#)]
21. Chen, Z.; Wang, X.; Cheng, X.; Yang, W.; Wu, Y.; Fu, F. Specifically and Visually Detect Methyl-Mercury and Ethyl-Mercury in Fish Sample Based on DNA-Templated Alloy Ag-Au Nanoparticles. *Anal. Chem.* **2018**, *90*, 5489–5495. [[CrossRef](#)] [[PubMed](#)]
22. Long, Y.J.; Li, Y.F.; Liu, Y.; Zheng, J.J.; Tang, J.; Huang, C.Z. Visual observation of the mercury-stimulated peroxidase mimetic activity of gold nanoparticles. *Chem. Commun.* **2011**, *47*, 11939–11941. [[CrossRef](#)] [[PubMed](#)]
23. Yan, L.; Chen, Z.P.; Zhang, Z.Y.; Qu, C.L.; Chen, L.X.; Shen, D.Z. Fluorescent sensing of mercury(II) based on formation of catalytic gold nanoparticles. *Analyst* **2013**, *138*, 4280–4283. [[CrossRef](#)] [[PubMed](#)]
24. Peng, C.-F.; Pan, N.; Xie, Z.-J.; Wu, L.-L. Highly sensitive and selective colorimetric detection of Hg<sup>2+</sup> based on the separation of Hg<sup>2+</sup> and formation of catalytic DNA–gold nanoparticles. *Anal. Methods* **2016**, *8*, 1021–1025. [[CrossRef](#)]
25. Wu, L.-L.; Wang, L.-Y.; Xie, Z.-J.; Xue, F.; Peng, C.-F. Colorimetric detection of Hg<sup>2+</sup> based on inhibiting the peroxidase-like activity of DNA–Ag/Pt nanoclusters. *RSC Adv.* **2016**, *6*, 75384–75389. [[CrossRef](#)]
26. Wang, C.I.; Huang, C.C.; Lin, Y.W.; Chen, W.T.; Chang, H.T. Catalytic gold nanoparticles for fluorescent detection of mercury(II) and lead(II) ions. *Anal. Chim. Acta* **2012**, *745*, 124–130. [[CrossRef](#)] [[PubMed](#)]
27. Kenduzler, E.; Ates, M.; Arslan, Z.; McHenry, M.; Tchounwou, P.B. Determination of mercury in fish otoliths by cold vapor generation inductively coupled plasma mass spectrometry (CVG-ICP-MS). *Talanta* **2012**, *93*, 404–410. [[CrossRef](#)] [[PubMed](#)]
28. Monteiro, A.d.C.P.; de Andrade, L.S.N.; Luna, A.S.; de Campos, R.C. Sequential quantification of methyl mercury in biological materials by selective reduction in the presence of mercury(II), using two gas–liquid separators. *Spectrochim. Acta Part B At. Spectrosc.* **2002**, *57*, 2103–2112. [[CrossRef](#)]
29. Yin, J.; Cao, H.; Lu, Y. Self-assembly into magnetic Co<sub>3</sub>O<sub>4</sub> complex nanostructures as peroxidase. *J. Mater. Chem.* **2012**, *22*, 527–534. [[CrossRef](#)]

30. Costas-Mora, I.; Romero, V.; Lavilla, I.; Bendicho, C. In situ building of a nanoprobe based on fluorescent carbon dots for methylmercury detection. *Anal. Chem.* **2014**, *86*, 4536–4543. [[CrossRef](#)] [[PubMed](#)]
31. Chatterjee, A.; Banerjee, M.; Khandare, D.G.; Gawas, R.U.; Mascarenhas, S.C.; Ganguly, A.; Gupta, R.; Joshi, H. Aggregation-Induced Emission-Based Chemodosimeter Approach for Selective Sensing and Imaging of Hg(II) and Methylmercury Species. *Anal. Chem.* **2017**, *89*, 12698–12704. [[CrossRef](#)] [[PubMed](#)]



© 2018 by the authors. Licensee MDPI, Basel, Switzerland. This article is an open access article distributed under the terms and conditions of the Creative Commons Attribution (CC BY) license (<http://creativecommons.org/licenses/by/4.0/>).